MEASUREMENTS OF LOCAL STRAIN VARIATION IN $Si_{1-x}Ge_x/Si$ HETEROSTRUCTURES

L. D. Bell, W. J. Kaiser, S. J. Manion, A. M. Milliken, W, T. Pike, and R. W. Fathauer

Center for Space Microelectronics Technology

Jet Propulsion Laboratory

California Institute of Technology

Pasadena, CA 91109

The energy splitting of the conduction-band minimum of $Si_{1-x}Ge_x$ due to strain has been directly measured by the application of BEEM spectroscopy to $Ag/Si_{1-x}Ge_x$ structures. Experimental values for this conduction-band splitting agree well with calculations. For $Au/Si_{1-x}Ge_x$, however, heterogeneity in the strain of the $Si_{1-x}Ge_x$ layer is introduced by deposition of the Au. This variation is attributed to species interdiffision, which produces a rough $Si_{1-x}Ge_x$ surface. Preliminary modeling indicates that the observed roughness is consistent with the strain variation measured by BEEM.

Interest in the strained-layer $Si_{1-x}Ge_x/Si$ system has been spurred in recent years by advances in growth technology, allowing the production of coherently strained epitaxial $Si_{1-x}Ge_x$ layers. Pseudomorphic $Si_{1-x}Ge_x/Si$ is a promising candidate for novel devices such as heterojunction bipolar transistors and long-wavelength infrared detectors. [1] In order to properly model the behavior of devices based on these materials, fundamental aspects of strained $Si_{1-x}Ge_x$ electronic structure must be directly measured. This paper describes the application of ballistic-electron-emission microscopy (BEEM) to a characterization of the effects of strain on the metal/$Si_{1-x}Ge_x/Si$ system.

$Si_{1-x}Ge_x$ layers were grown on Si substrates by molecular-beam epitaxy (MBE). These layers were thinner than the critical thickness for the introduction of misfit dislocations; they therefore remained fully strained and pseudomorphic with the underlying Si lattice. The unstrained $Si_{1-x}Ge_x$ lattice constant is slightly larger than that of Si; therefore the pseudomorphic layer is under compressive strain in the plane of the layer. Tensile strain is imposed perpendicular to the layer, due to the Poisson effect. The resulting distortion of the $Si_{1-x}Ge_x$ lattice modifies the band structure of the material.[3,4] The light- and heavy-hole valence bands are split at the zone center. In addition, the silicon-like six-fold-degenerate conduction-band minimum is split by this strain into two sets of minima with differing energies. The energies of the four in-plane minima are lowered, and the energies of the two out-of-plane minima are raised, The dependence of this conduction-band splitting on Ge alloy fraction has been calculated[3,4]. A measurement of this splitting by electron-energy-loss spectroscopy has recently been reported[5] for a thin $Si_{1-x}Ge_x$ quantum well layer.

BEEM utilizes scanning tunneling microscopy (STM) to inject electrons into a heterostructure by vacuum tunneling from the STM tip. By varying the tip-sample voltage, the energies of the electrons injected into the metal maybe controlled, and a spectroscopy of transport may be performed. BEEM has previously been used to characterize Schottky barrier

height[7,8] (SBH) and carrier transport through metal/semiconductor structures[9-12]. Additional aspects of the conduction band structure have also been characterized. 1 n the case of GaAs, the satellite minima at the L and X points have been directly observed using BEEM[2]. Observation of these minima in the BEEM spectra is enabled by scattering during the electron transport process through the metal and across the metal/semiconductor interface, which widens the initially narrow angular distribution produced by tunneling.

The growth and preparation of the samples have been discussed previously, [13] Samples were grown with nominally pseudomorphically strained (below the critical thickness for the introduction of misfit dislocations) intrinsic $Si_{1-x}Ge_x$ layers. The strained layers were 50 nm thick, with either x=O. 18 or x=0.25. BEEM measurements were performed in a nitrogen-purged glove-box, both at room temperature and at 77K. Due to the large leakage currents in some samples, 77K was necessary for acquisition of low-noise spectra.

$Au/Si_{1-x}Ge_x/Si$ samples were prepared for BEEM using $Si_{.82}Ge_{.18}$ and $Si_{.75}Ge_{.25}$ MBE layers, with evaporated Au layers 10 nm thick. In contrast to Au/Si(1 00) BEEM spectra, which show a single threshold and are fit well by a simple phase-space model[2,14], the $Au/Si_{1-x}Ge_x/Si$ BEEM spectra usually exhibited two thresholds. Similar to the case of GaAs, these two thresholds correspond to the onset of electron transmission into two sets of states in the $Si_{1-x}Ge_x$ layer. These states are comprised of the two sets of conduction-band minima which are split by strain. Unexpectedly, the energy difference of these two thresholds was found to vary from spectrum to spectrum in the range 0-350 meV, with a roughly uniform distribution of splittings within this range. A BEEM spectrum representative of one of the larger values of this splitting is shown in Fig. 1a. The two-threshold nature of the spectrum is apparent, with a separation in this case of about 300 mV. For comparison, a spectrum which exhibited a single threshold is shown in Fig lb, with a one-threshold fit also plotted.

The BEEM results show that there is a large spatial variation in strain of the $Si_{.75}Ge_{.25}$ layer, This variation was observed for the $Si_{.82}Ge_{.18}$ samples as well. In both cases, the energy difference of the two BEEM thresholds varied from zero to about twice the calculated value. Several possibilities exist for the cause of this heterogeneity. A variation in alloy fraction of the $Si_{1-x}Ge_x$ layer would produce a corresponding variation in the strain of the layer, and areas in which no splitting was observed would correspond to areas where the Ge fraction and the strain were nearly zero. A test of this premise was performed using BEEM spectra which showed only a single threshold. These spectra were compiled, and the average SBH was calculated for each alloy fraction. The results indicate a steady decrease in SBH with nominal alloy fraction. [13] If these spectra represented areas where the Ge fraction was nearly zero, a SBH which is independent of the nominal bulk alloy fraction would be expected.

A second possible mechanism is the presence of an intrinsic structural variation of the $Si_{1-x}Ge_x$ layer. Such a variation has been observed in the form of a periodic strain relaxation [5,16]. This relaxation produces a corrugated surface, with enhanced strain in the troughs and reduced strain at the crests. This corrugation has been observed to have a period of a few hundred nm and an amplitude of several nm, although these parameters depend on Ge fraction and layer thickness. In order to ascertain the presence of such a relaxation, high-resolution cross-sectional TEM was performed on the $Si_{.82}Ge_{.18}$ material. The results are shown in Fig, 2a. It can be seen that the $Si_{1-x}Ge_x$ surface is flat, with no evidence of a relaxation such as that observed in ref. 16.

Since characterization of the bare $Si_{1-x}Ge_x$ surface indicated a uniform pseudomorphic layer, the possibility that the Au produces a heterogeneity that is not present on the as-grown layer was investigated. Cross-sectional TEM performed on a completed $Au/Si_{1-x}Ge_x/Si$ structure confirms that this is the case. A representative image is shown in Fig. 2b. It is apparent that the $Si_{1-x}Ge_x$ surface has been dramatically roughened by the Au

deposition. This roughness appears with an amplitude on the order of 2 or 3 nm, and on a length scale of20 to 50 nm.

In order to compare the effect of another metal to that of Au, a series of samples was fabricated utilizing a metal bilayer consisting of 8 nm of Ag, capped by 8 nm of Au. The top Au layer was necessary to prevent oxidation of the Ag. The lower SBH produced by Ag, coupled with the somewhat large leakage current which was characteristic of all the metal/$Si_{1-x}Ge_x$ structures, required that all measurements on the Ag systems be performed at 77K. The separations between thresholds obtained from BEEM spectroscopy of these samples are shown in Fig. 3. In contrast to the Au/$Si_{1-x}Ge_x$ case, BEEM measurements of the Ag/$Si_{1-x}Ge_x$ structures yielded values of conduction band splitting which were uniform and in good agreement with theory.[4] TEM imaging of these samples confirmed that, as expected, the $Si_{1-x}Ge_x$ roughening which occurred with Au was absent in the Ag case, One such image is shown in Fig. 2c. These results strongly indicate a correlation between the $Si_{1-x}Ge_x$ roughening and the variation in strain observed by BEEM.

The deposition of Au onto Si is known to produce a strong intermixing reaction, even at room temperature. Although most work has been done on Si(11 1), Au/Si(100) has also been studied[17]. It has been shown that an intermixed layer may format the interface, which can be several nanometers thick. [18] This intermixed region can be non-uniform, depending on trace contamination remaining at the Au/Si interface 8, and perhaps on Au crystallite orientation.

The observed roughness at the Au/$Si_{1-x}Ge_x$ interface provides an explanation for the variation in conduction-band splitting observed with BEEM. Pidduck et al. [16] have discussed a relaxation of the $Si_{1-x}Ge_x$ layer for certain growth parameters. The authors argued that in these cases it becomes energetically favorable for the surface to assume a periodic corrugation on a lateral scale of hundreds of nanometers. As a result of this relaxation, strain is decreased in the

neighborhood of the peaks and enhanced in the troughs, Although the roughness observed in the case of $Au/Si_{1-x}Ge_x$ is of a different nature, involving removal of material by difision, the same qualitative arguments for variation of strain apply. Partial removal of lateral constraint around high areas allows partial relaxation of strain in these regions, and this relaxation induces strain enhancement in the low areas.

It is necessary to show that the variation of conduction-band splittings derived from BEEM data is consistent with the degree of roughness observed by TEM. Since the strain variation induced by the surface roughness is of arbitrary magnitude and direction, numerical methods were required for this calculation. The lattice-matched $Si_{1-x}Ge_x/Si$ system is described well by elasticity theory[3]; therefore, a finite-element implementation of elasticity was chosen to model the problem. The derived strains in the layer were then used to calculate conduction-band positions and splittings.

The equilibrium strain configuration of the $Si_{1-x}Ge_x$ layer was determined by the solution to a two-dimensional finite-element system. A mesh of triangular elements was used, and a solution was obtained when net force on each element node was equal to zero. This array was used to represent the $Si_{1-x}Ge_x$ layer of our samples, which was nominally 50 nm thick. Periodic boundary conditions were used laterally, with the last node of a row mathematically connected to the first node of the row. A rigid Si substrate lattice was used to fix the bottom row of the grid. Since the degree of roughness was determined by reference to Fig 2b, initial strain in the layer was chosen to be that appropriate for $Si_{0.82}Ge_{0.18}$ lattice-matched to Si. Elastic constants for Si and Ge were linearly interpolated to arrive at constants for the alloy. Strain in the third dimension was fixed at a constant value.

Table I lists the relevant lattice constants a and elastic constants for Si and Ge.[19] The derived Poisson ratio v is also shown, Values for $Si_{0.82}Ge_{0.18}$ are linear interpolations.

TABLE I

Parameter	Si	Ge	$Si_{0.82}Ge_{0.18}$
a (rim)	0.5431	0.5658	0.5472
c_{11} (Mbar)	1.656	1.285	1.589
c_{12} (Mbar)	0.639	0.483	0.611
C44 (Mbar)	0.795	0.680	0.774
$\nu=c_{12}/(c_{11}+c_{12})$	0.278	0.273	0.278

The lattice constants in Table I yield a bulk value for in-plane uniaxial strain of

$$e_{xx} = (a_{Si} - a_{SiGe}) / a_{SiGe} = -0.749\% \quad (1)$$

with the sign indicating compressive strain. Strain in the third dimension (normal to the grid) was maintained at $e_{yy} = -0.749°/0$. Resulting extension in the direction normal to the plane of the layer is

$$e_{zz} = -2\frac{c_{12}}{c_{11}} \cdot e_{xx} = 0.576\%. \quad (2)$$

The finite-element grid was initialized using these values.

In order to calculate band splittings, uniaxial contributions to band positions are calculated. The deformation potential for this contribution is Ξ_u, and the energy shift for a given conduction-band minimum, relative to the weighted average, is[3]

$$E_u^i = \Xi_u\left[\{\hat{a}_i \hat{a}_i\} : \ddot{e} - \tfrac{1}{3}(\ddot{1} : \ddot{e})\right] \tag{3}$$

where $\hat{a}_i$ is the unit vector in the direction of the i^{th} conduction band minimum, and $\{\hat{a}_i \hat{a}_i\}$ represents a dyadic product. Therefore,

$$E_u^x = \Xi_u\left[+\tfrac{2}{3}e_{xx} - \tfrac{1}{3}e_{yy} - \tfrac{1}{3}e_{zz}\right] \tag{4a}$$

$$E_u^y = \Xi_u\left[-\tfrac{1}{3}e_{xx} + \tfrac{2}{3}e_{yy} - \tfrac{1}{3}e_{zz}\right] \tag{4b}$$

$$E_u^z = \Xi_u\left[-\tfrac{1}{3}e_{xx} - \tfrac{1}{3}e_{yy} + \tfrac{2}{3}e_{zz}\right]. \tag{4c}$$

For in-plane compressive strain of the SiGe layer (e_{xx} and e_{yy} negative) energies of [001] minima will in general be raised, and the energies of [100] and [01 O] minima will be lowered.

It is important to note that, since the observed variation in strain is attributed to surface roughness, all three components of strain will in general be different. This would produce a BEEM spectrum which exhibits three separate thresholds. In practice, however, it is more difficult to reliably resolve three thresholds than two. In order to clearly distinguish the three thresholds, it is necessary to have large strain and also to have the intermediate threshold roughly equidistant between the other two. Since this is a relatively uncommon situation, we have parameterized the spectra in this work with two-threshold fits. While this may underestimate the separation between the highest and lowest of three thresholds, it is unlikely to overestimate.

The deformation potential Ξ_u used for Si and Ge are 9.16 eV and 9.42 eV, respectively.[4] A linear interpolation yields 9.21 eV for $Si_{0.82}Ge_{0.18}$. These deformation potentials are for the A minima, since for x=O. 18 this minimum is lowest in energy for all values of strain. For $Si_{0.82}Ge_{018}$, Eqs. 4 and the interpolated value of Ξ_u yield a bulk value for conduction-band splitting of 122 meV.

The initial modeling of the roughened interface has been performed using a sinusoidal profile for the SiGe surface. The amplitude and period were selected to approximate the profile observed by TEM. SiGe layer thickness as determined from cross-sectional TEM was approximately 56 nm; amplitude and period, A = 2.05 nm and P = 56 nm, respectively, were assigned for the sinusoidal profile. Other amplitude and period values were also investigated.

Figures 4a and 4b show the sinusoidal surface. Using this profile, the finite-element model was used to obtain components of strain at the surface. The strain components e_{xx} and e_{zz} are plotted in Figs. 5b and 5c. Also shown for reference are the bulk values of the strain components. Note that both components of strain are distinctly non-sinusoidal and are not symmetric about the bulk values. Figure 4C shows the conduction-band splitting along the surface, derived from Eqs. 4 using the calculated surface strains, The variation in splitting is from 0.095 eV to 0.144 eV.

Since a two-dimensional model is used for the strain calculation, it is limited to the imposition of a constant strain in the third dimension. However, the roughness at the $Au/Si_{1-x}Ge_x$ interface extends to both lateral dimensions, and the TEM micrograph of Fig. 2b may be thought to represent the typical roughness in any lateral direction, One aim of these calculations is to derive an expected maximum and minimum splitting consistent with the observed roughness. Although the two-dimensional roughness cannot be determined from the TEM images, the effect can be estimated by imposing a constant strain e_{yy} in the other lateral

direction, equal to the maximum or minimum value of e_{xx}, and performing a separate calculation for each case. This procedure yields a slightly increased maximum splitting valueofO.151 eV and a slightly decreased minimum of 0.087 eV; these corrected values are also indicated in Fig. 4c.

In general, the maximum and minimum strains at the surface depend to first order only on the amplitude-to-period ratio (A/P) of the sinusoidal roughness, as long as the strain distortion imposed by the roughness decays sufficiently quickly with depth. In practice this seems to be true for P less than the layer thickness. Several A/P values were modeled, and the results for the maximum and minimum conduction-band splittings are plotted in Fig. 6. It can be seen that the maximum and minimum are not symmetric about the bulk splitting value, a characteristic which is also apparent in Figs. 4 and 5. This is reasonable, since the lateral constraints of elements at the bottom of surface troughs are not directly affected by roughness, but only indirectly by the secondary effect of the relaxation of high areas.

Since the actual surface has areas of larger curvature than the model sinusoidal surface, it is expected that calculations for the actual surface will show a larger range of strains than those for this idealized surface. These calculations are currently underway. In conclusion, the conduction-band splitting of strained Si and $Si_{1-x}Ge_x$ has been directly measured using BEEM spectroscopy. For the case of Ag on $Si_{1-x}Ge_x$, the energy splitting is uniform, with values which agree well with calculations. Deposition of Au on $Si_{1-x}Ge_x$, however, produces a large degree Of spatial heterogeneity in the strain of the $Si_{1-x}Ge_x$ layer. This characteristic is also seen On strained Si, and appears to be due to the intermixing of Au and Si, leading to a roughened interface and heterogeneous strain. The calculated band splittings of an idealized $Si_{1-x}Ge_x$ surface are in reasonable agreement with measured BEEM splittings, indicating that the observed roughness is the probable cause for the variation in observed splittings. Further calculations for a more realistic surface should improve on this agreement. These results emphasize the importance of a characterization and understanding of the completed metal/semiconductor heterostructure.

The research described in this paper was performed by the Center for Space Microelectronics Technology, Jet Propulsion Laboratory, California Institute of Technology, and was jointly sponsored by the Office of Naval Research and the Ballistic Missile Defense Organization / Innovative Science and Technology Office through an agreement with the National Aeronautics and Space Administration (NASA).

REFERENCES

1. S. C. Jain and W. Hayes, Semicond. *Sci. Technol. 6,547 (1991).*
2. W, J. Kaiser and L. D. Bell, *Phys. Rev. Lett. 60, 1406 (1988);* L. D. Bell and W. J. Kaiser, *Phys. Rev. Lett. 61,2368 (1988).* For a more complete review of BEEM, see L. D. Bell, W. J. Kaiser, M. H. Hecht, and L. C. Davis, in ***Scanning Tunneling Microscopy,*** edited by J. A. Stroscio and W. J. Kaiser (Academic Press, San Diego, 1993), pp. 307-348.
3. R. People, *Phys. Rev. B 32, 1405 (1985).*
4. Chris G. Van de Wane and Richard M. Martin, *Phys. Rev. B* 34, 5621 (1986).
5. P. E. Batson and J. F. Morar, *Phys. Rev. Lett. 71, 609(1993).*
6. G. Binnig, H. Rohrer, Ch. Gerber, and E. Weibel, *Phys. Rev. Lett.* 49, 57 (1982).
7. A. Fernandez, H. D. Hallen, T. Huang, R. A. Buhrman, and J. Silcox, *J. Vat. Sci. Technol. B 9, 590 (1991).*
8. M, Prietsch and R, Ludeke, *Phys. Rev. Lett. 66,2511* (1 991).
9. L. D. Bell, M. H. Hecht, W. J. Kaiser, and L. C. Davis, *Phys. Rev. Lett.* 64,2679 (1990).
10. A. M. Milliken, S. J. Manion, W. J. Kaiser, L. D. Bell, and M. H. Hecht, *Phys. Rev. B 46, 12826 (1992).*
11. R. Ludeke, *Phys. Rev. Lett. 70,214 (1993).*
12. A. Bauer, M. T. Cuberes, M. Prietsch, and G, Kaindl, *Phys. Rev. Lett.* **71, 149 (1993).**
13. L. D. Bell, A, M. Milliken, S. J. Manion, W. J. Kaiser, R. W. Fathauer, and W. T. Pike, *Phys. Rev. B* 50,8082 (1994).
14. E. Y. Lee and L. J. Schowalter, *Phys. Rev. B* 45,6325 (1992).
15. A. G. Cullis, D. J. Robbins, A. J. Pidduck, and P, W. Smith, *J. Cryst. Growth 123, 333 (1992).*
16. A. J. Pidduck, D. J. Robbins, A. G, Cullis, W. Y. Leong, and A. M. Pitt, *Thin Solid Films 222,78 (1992).*
17. M. Hanbucken, Z. Imam, J. J. Metois, and G. LeLay, *Surf. Sci.* 162, 628(1985).

18. Z. Ma and L. H. Allen, *Phys.* Rev. *B* 48, 15484 (1993).

19. ***CRC Handbook of Materials Science, Vol. III,*** edited by Charles T. Lynch (CRC Press, Cleveland, 1975).

FIGURES

1. (a) Experimental BEEM spectrum of collector current (I_C) versus tunnel voltage for a $Au/Si_{.75}Ge_{.25}/Si(100)$ heterostructure. Tunnel current for this spectrum was 3 nA. The data are shown by circles. Also plotted are two theoretical spectra which have been fit to the data. The first (dashed line) fits only the low-voltage portion ($V < 1.1V$) with a single threshold; the other fit (solid line) is over a larger range (to 1.6V) using a two-threshold model. The extracted thresholds for the two-threshold fit are separated by about 0.30 V. (b) BEEM I_c-V spectrum, taken on a sample identical to that in (a), showing only a single threshold. Tunnel current for this spectrum was 2 nA. Also plotted is a one-threshold fit to the data (solid line).

2. High-resolution cross-sectional TEM images of $Si_{1-x}Ge_x/Si$ structures. The SiGe/Si interface is out of the field of view in all three images. (a) Image of the as-grown $Si_{.75}Ge_{.25}$ material. (b) Image of a $Si_{.82}Ge_{.18}$ sample with an evaporated Au layer of nominal thickness 10 nm. (c) Image of a $Si_{.82}Ge_{.18}$ sample with 8 nm of evaporated Ag, capped with 8 nm of Au. Nonuniform thinning during sample preparation is responsible for the dark area in the bottom right comer.

3. Conduction-band splitting for $Au/Ag/Si_{1-x}Ge_x/Si(100)$. The experimental points (circles) are derived from the fitted thresholds of the corresponding BEEM spectra. Also plotted (square) is the derived splitting for $Au/Ag/Si(strained)/Si_{1-x}Ge_x(relaxed)$ at x=.25. The calculated dependence (line) is from Eqs. 4.

4. (a, b) Sinusoidal surface profile used in elasticity calculations. y=O corresponds to the $Si_{.82}Ge_{.18}/Si$ interface. (c) Calculated conduction-band splitting along this surface. The upper and lower dashed lines represent maximum and minimum values of strain after correction for roughness in two dimensions. The middle dashed line indicates the bulk splitting value.

5. (a) Sinusoidal surface profile used in elasticity calculations, as in Fig. 4b. (b, c) Calculated strain components e_{xx} and e_{zz} along this surface. The dashed lines indicate the bulk values of the strain components.

6. Calculated maximum and minimum splittings at the surface of the $Si_{.82}Ge_{.18}$ layer as a function of amplitude/period ratio (A/P) of the sinusoidal surface roughness. These values have been corrected to estimate the effect of roughness in two dimensions, as described in the text. Also shown for reference is the bulk splitting value (dashed line).

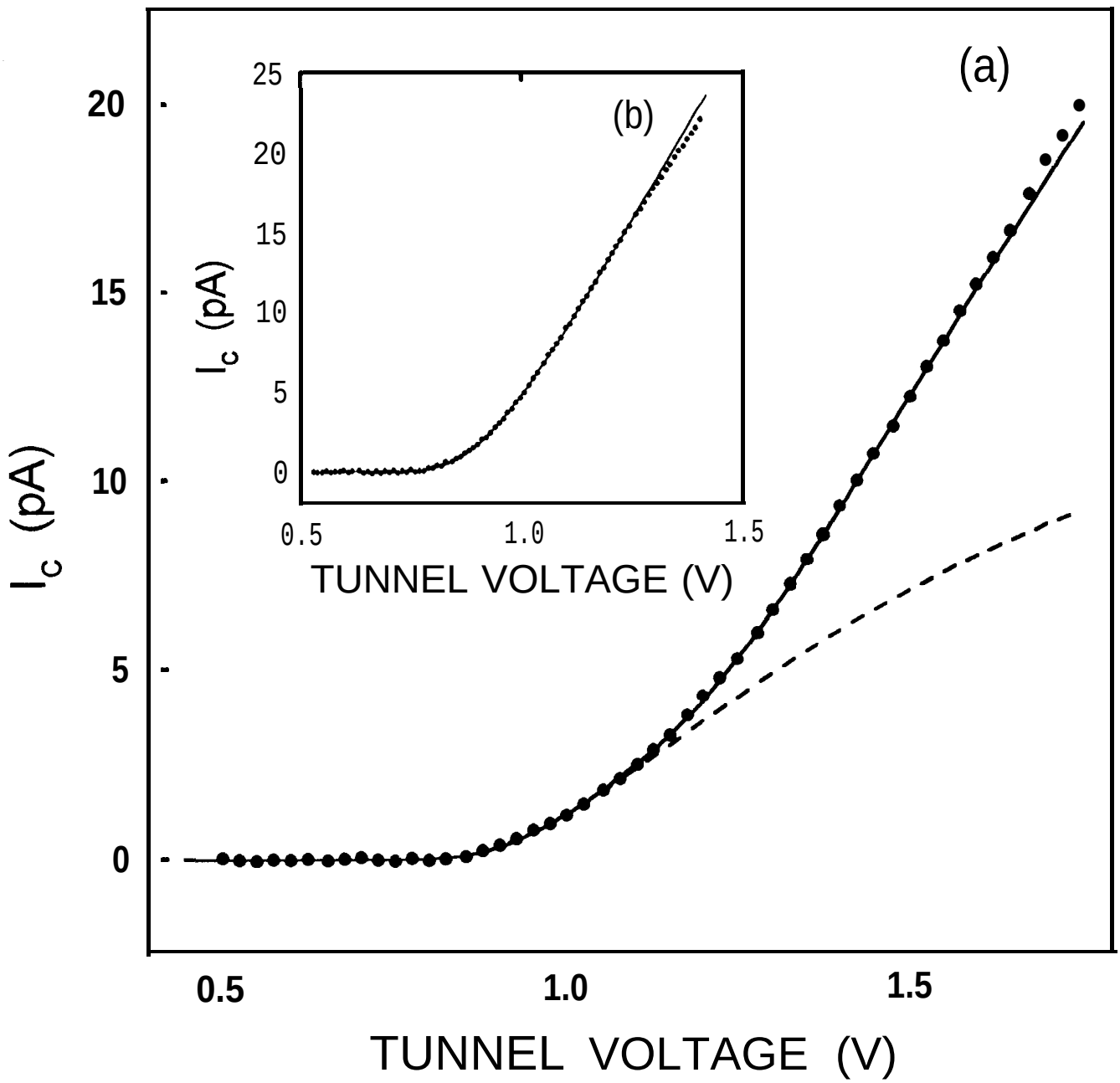

Fig 1

a

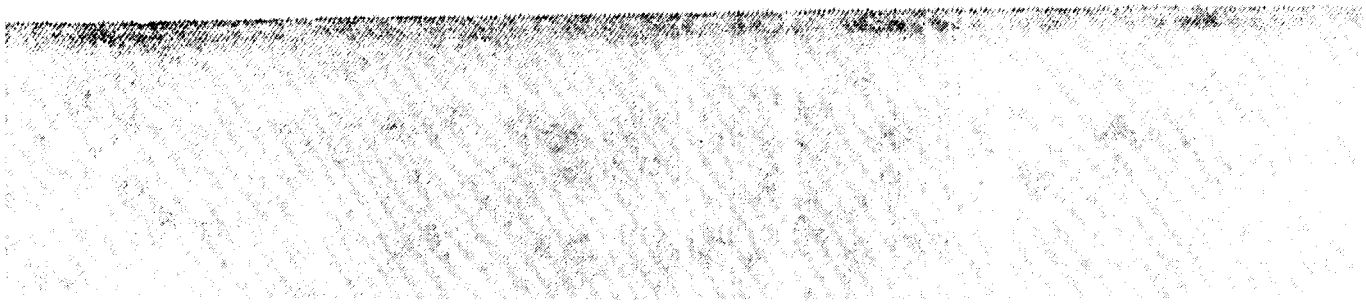

b

c

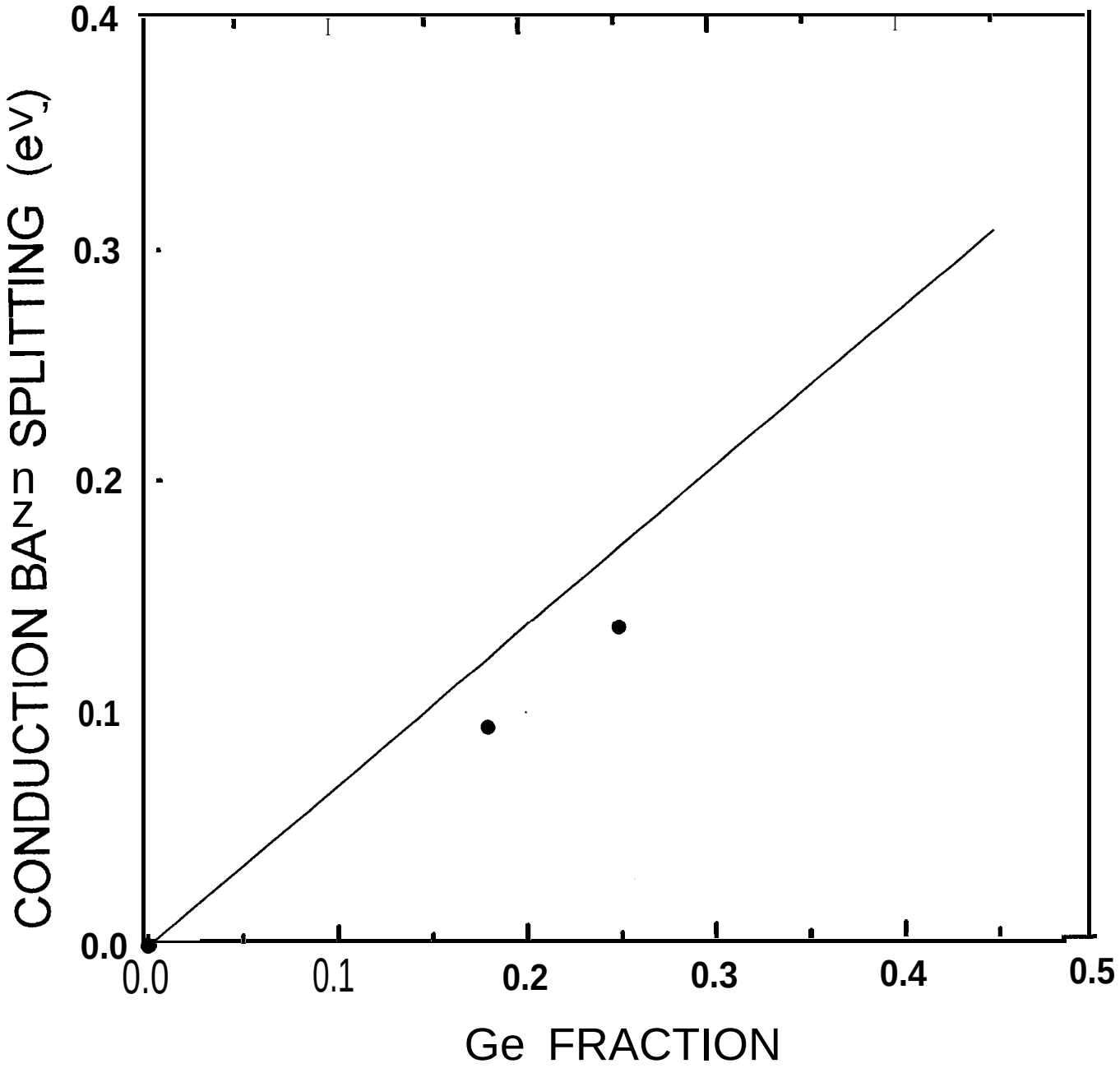
0.4
0.3
0.2
0.1
0.0
CONDUCTION BAND SPLITTING (eV)
0.0
0.1
0.2
0.3
0.4
0.5
Ge FRACTION

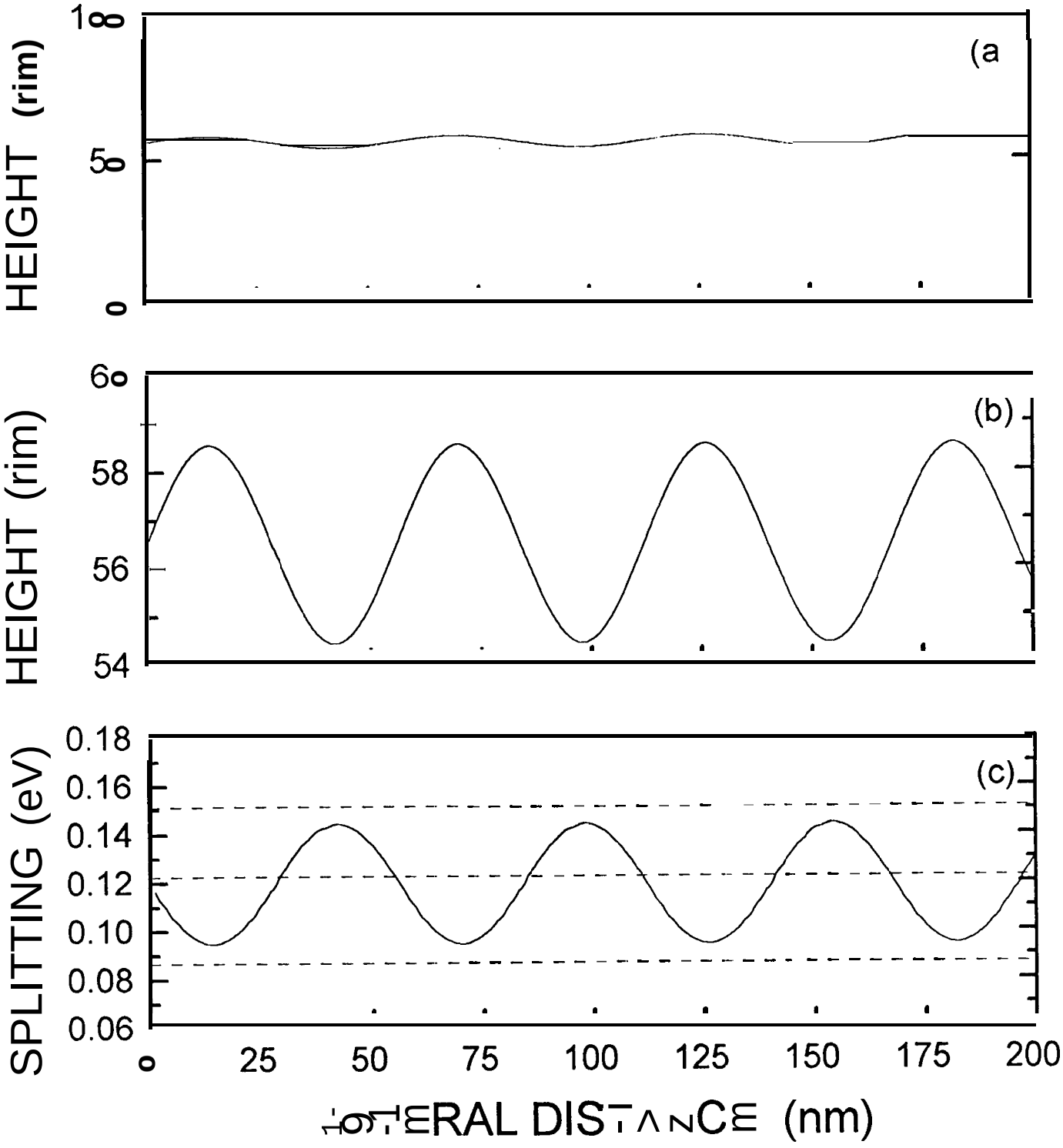
HEIGHT (rim)
10
5
0
(a)
HEIGHT (rim)
60
58
56
54
(b)
SPLITTING (eV)
0.18
0.16
0.14
0.12
0.10
0.08
0.06
(c)
0
25
50
75
100
125
150
175
200
LATERAL DISTANCE (nm)

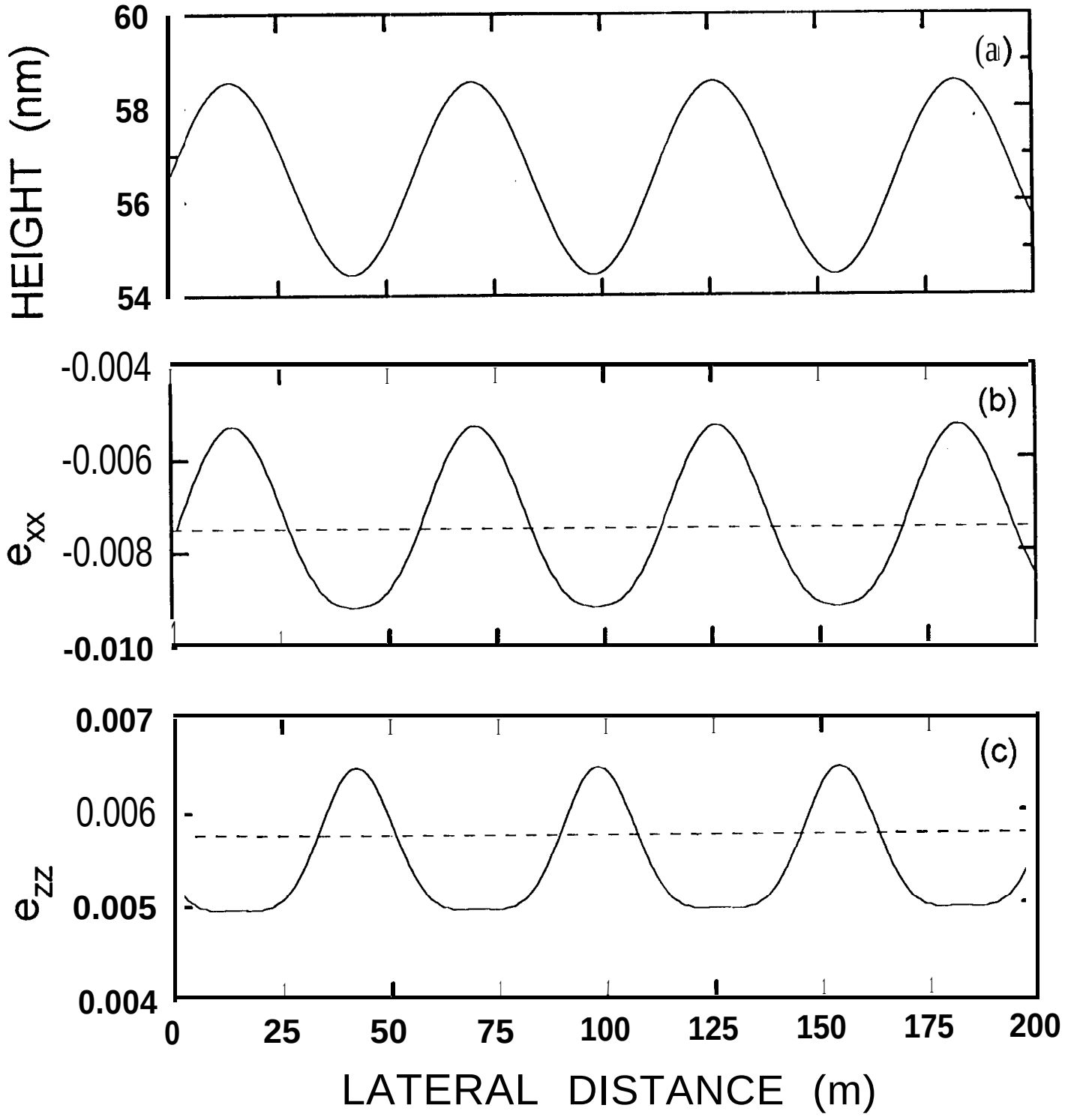
HEIGHT (nm)
60
58
56
54
(a)
e_{xx}
-0.004
-0.006
-0.008
-0.010
(b)
e_{zz}
0.007
0.006
0.005
0.004
(c)
0
25
50
75
100
125
150
175
200
LATERAL DISTANCE (m)

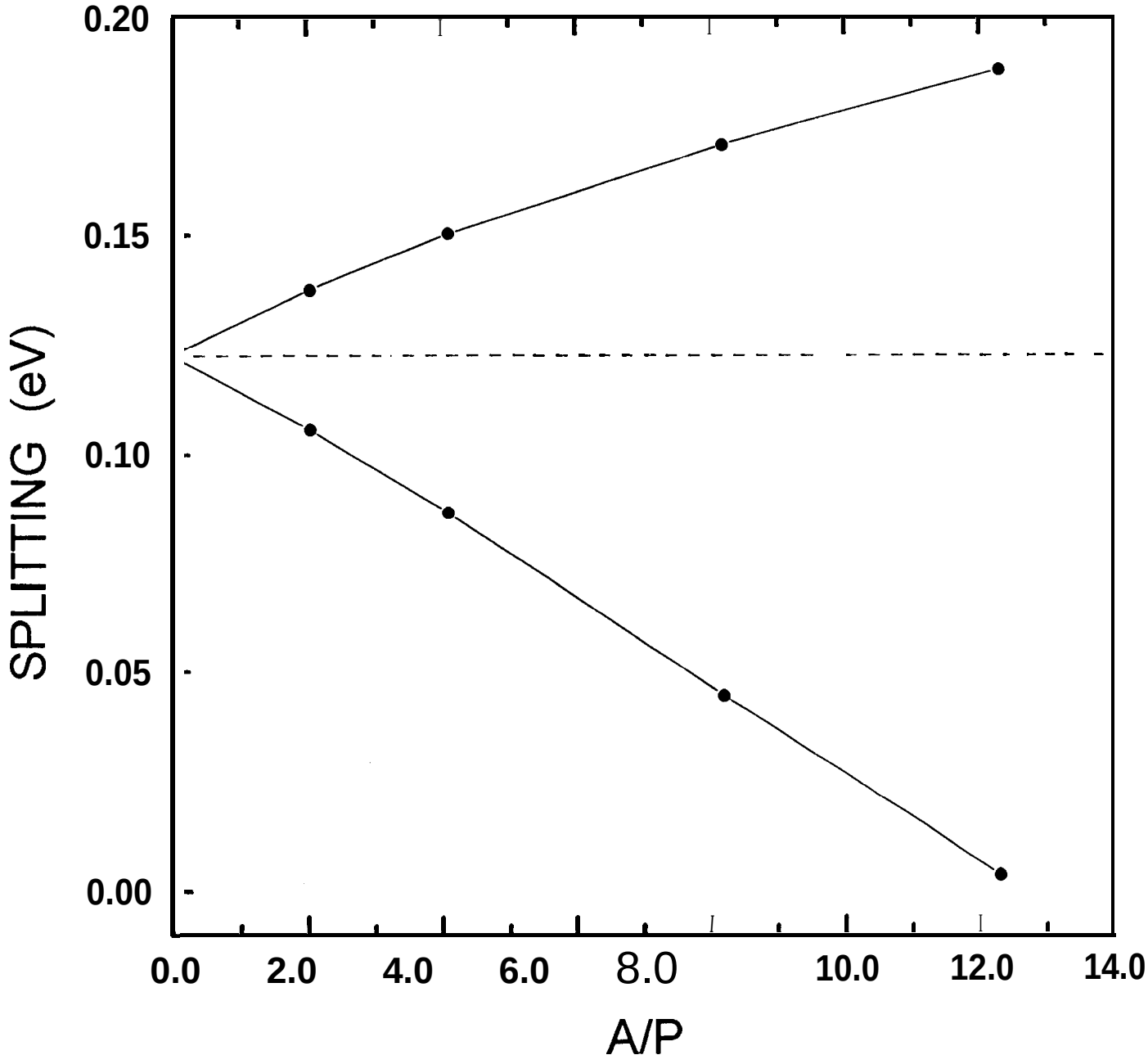
0.20
0.15
0.10
0.05
0.00
SPLITTING (eV)
0.0
2.0
4.0
6.0
8.0
10.0
12.0
14.0
A/P

MEASUREMENTS OF LOCAL STRAIN VARIATION IN $Si_{1-x}Ge_x$/Si HETEROSTRUCTURES

L. D. Bell, W, J. Kaiser, S. J. Manion, A. M. Milliken, W. T. Pike, and R, W. Fathauer

Center for Space Microelectronics Technology

Jet Propulsion Laboratory

California Institute of Technology

Pasadena, CA 91109

The energy splitting of the conduction-band minimum of $Si_{1-x}Ge_x$ due to strain has been directly measured by the application of BEEM spectroscopy to $Ag/Si_{1-x}Ge_x$ structures. Experimental values for this conduction-band splitting agree well with calculations. For $Au/Si_{1-x}Ge_x$, however, heterogeneity in the strain of the $Si_{1-x}Ge_x$ layer is introduced by deposition of the Au. This variation is attributed to species interdifision, which produces a rough $Si_{1-x}Ge_x$ surface. Preliminary modeling indicates that the observed roughness is consistent with the strain variation measured by BEEM.

Interest in the strained-layer $Si_{1-x}Ge_x/Si$ system has been spurred in recent years by advances in growth technology, allowing the production of coherently strained epitaxial $Si_{1-x}Ge_x$ layers. Pseudomorphic $Si_{1-x}Ge_x/Si$ is a promising candidate for novel devices such as heterojunction bipolar transistors and long-wavelength infrared detectors, [1] In order to properly model the behavior of devices based on these materials, fundamental aspects of strained $Si_{1-x}Ge_x$ electronic structure must be directly measured. This paper describes the application of ballistic-electron-emission microscopy (BEEM) to a characterization of the effects of strain on the metal/$Si_{1-x}Ge_x/Si$ system,

$Si_{1-x}Ge_x$ layers were grown on Si substrates by molecular-beam epitaxy (MBE). These layers were thinner than the critical thickness for the introduction of misfit dislocations; they therefore remained fully strained and pseudomorphic with the underlying Si lattice. The unstrained $Si_{1-x}Ge_x$ lattice constant is slightly larger than that of Si; therefore the pseudomorphic layer is under compressive strain in the plane of the layer. Tensile strain is imposed perpendicular to the layer, due to the Poisson effect. The resulting distortion of the $Si_{1-x}Ge_x$ lattice modifies the band structure of the material.[3,4] The light- and heavy-hole valence bands are split at the zone center. In addition, the silicon-like six-fold-degenerate conduction-band minimum is split by this strain into two sets of minima with differing energies. The energies of the four in-plane minima are lowered, and the energies of the two out-of-plane minima are raked. The dependence of this conduction-band splitting on Ge alloy fraction has been calculated[3,4]. A measurement of this splitting by electron-energy-loss spectroscopy has recently been reported[5] for a thin $Si_{1-x}Ge_x$ quantum well layer.

BEEM utilizes scanning tunneling microscopy[6] (STM) to inject electrons into a heterostructure by vacuum tunneling from the STM tip. By varying the tip-sample voltage, the energies of the electrons injected into the metal maybe controlled, and a spectroscopy of transport may be performed. BEEM has previously been used to characterize Schottky barrier

height[7,8] (SBH) and carrier transport through metal/semiconductor structures[9-12]. Additional aspects of the conduction band structure have also been characterized. In the case of GaAs, the satellite minima at the L and X points have been directly observed using BEEM[2]. Observation of these minima in the BEEM spectra is enabled by scattering during the electron transport process through the metal and across the metal/semiconductor interface, which widens the initially narrow angular distribution produced by tunneling.

The growth and preparation of the samples have been discussed previously. [13] Samples were grown with nominally pseudomorphically strained (below the critical thickness for the introduction of misfit dislocations) intrinsic $Si_{1-x}Ge_x$ layers. The strained layers were 50 nm thick, with either x=O. 18 or x=0.25. BEEM measurements were performed in a nitrogen-purged glove-box, both at room temperature and at 77K. Due to the large leakage currents in some samples, 77K was necessary for acquisition of low-noise spectra.

$Au/Si_{1-x}Ge_x/Si$ samples were prepared for BEEM using $Si_{.82}Ge_{.18}$ and $Si_{.75}Ge_{.25}$ MBE layers, with evaporated Au layers 10 nm thick. In contrast to Au/Si(100) BEEM spectra, which show a single threshold and are fit well by a simple phase-space model[2,14], the $Au/Si_{1-x}Ge_x/Si$ BEEM spectra usually exhibited two thresholds. Similar to the case of GaAs, these two thresholds correspond to the onset of electron transmission into two sets of states in the $Si_{1-x}Ge_x$ layer. These states are comprised of the two sets of conduction-band minima which are split by strain. Unexpectedly, the energy difference of these t wo thresholds was found to vary from spectrum to spectrum in the range 0-350 meV, with a roughly uniform distribution of splittings within this range. A BEEM spectrum representative of one of the larger values of this splitting is shown in Fig. 1a. The two-threshold nature of the spectrum is apparent, with a separation *in* this case of about 300 mV. For comparison, a spectrum which exhibited a single threshold is shown in Fig lb, with a one-threshold fit also plotted.

The BEEM results show that there is a large spatial variation in strain of the $Si_{.75}Ge_{.25}$ layer. This variation was observed for the $Si_{.82}Ge_{.18}$ samples as well. In both cases, the energy difference of the two BEEM thresholds varied fi om zero to about than twice the calculated value. Several possibilities exist for the cause of this heterogeneity. A variation in alloy fraction of the $Si_{1-x}Ge_x$ layer would produce a comesponding variation in the strain of the layer, and areas in which no splitting was observed would correspond to areas where the Ge fraction and the strain were nearly zero, A test of this premise was performed *using* BEEM spectra which showed only a single threshold. These spectra were compiled, and the average SBH was calculated for each alloy fraction. The results indicate a steady decrease in SBH with nominal alloy fraction. [13] If these spectra represented areas where the Ge fraction was nearly zero, a SBH which is independent of the nominal bulk alloy fraction would be expected.

A second possible mechanism is the presence of an intrinsic structural variation of the $Si_{1-x}Ge_x$ layer. Such a variation has been observed in the form of a periodic strain relaxation[15,16]. This relaxation produces a corrugated surface, with enhanced strain in the troughs and reduced strain at the crests. This corrugation has been observed to have a period of a few hundred nm and an amplitude of several nm, although these parameters depend on Ge fraction and layer thickness. In order to ascertain the presence of such a relaxation, high-resolution cross-sectional TEM was performed on the $Si_{.82}Ge_{.18}$ material. The results are shown in Fig, 2a. It can be seen that the $Si_{1-x}Ge_x$ surface is flat, with no evidence of a relaxation such as that observed in ref. 16.

Since characterization of the bare $Si_{1-x}Ge_x$ surface indicated a uniform pseudomorphic layer, the possibility that the Au produces a heterogeneity that is not present on the as-grown layer was investigated. Cross-sectional TEM performed on a completed $Au/Si_{1-x}Ge_x/Si$ structure confirms that this is the case, A representative image is shown in Fig. 2b. It is apparent that the $Si_{1-x}Ge_x$ surface has been dramatically roughened by the Au

deposition, This roughness appears with an amplitude on the order of 2 or 3 nm, and on a length scale of20 to 50 nm.

In order to compare the effect of another metal to that of Au, a series of samples was fabricated utilizing a metal bilayer consisting of 8 nm of Ag, capped by 8 nm of Au. The top Au layer was necessary to prevent oxidation of the Ag. The lower SBH produced by Ag, coupled with the somewhat large leakage current which was characteristic of all the metal/$Si_{1-x}Ge_x$ structures, required that all measurements on the Ag systems be performed at 77K. The separations between thresholds obtained from BEEM spectroscopy of these samples are shown in Fig. 3. In contrast to the $Au/Si_{1-x}Ge_x$ case, BEEM measurements of the $Ag/Si_{1-x}Ge_x$ structures yielded values of conduction band splitting which were uniform and in good agreement with theory.[4] TEM imaging of these samples confirmed that, as expected, the $Si_{1-x}Ge_x$ roughening which occurred with Au was absent in the Ag case. One such image is shown in Fig. 2c. These results strongly indicate a correlation between the $Si_{1-x}Ge_x$ roughening and the variation in strain observed by BEEM.

The deposition of Au onto Si is known to produce a strong intermixing reaction, even at room temperature. Although most work has been done on Si(111), Au/Si(100) has also been studied[17]. It has been shown that an intermixed layer may form at the interface, which can be several nanometers thick, [18] This intermixed region can be non-uniform, depending on trace contamination remaining at the Au/Si interfaces, and perhaps on Au crystallite orientation.

The observed roughness at the $Au/Si_{1-x}Ge_x$ interface provides an explanation for the variation in conduction-band splitting observed with BEEM. Pidduck et al. [16] have discussed a relaxation of the $Si_{1-x}Ge_x$ layer for certain growth parameters. The authors argued that in these cases it becomes energetically favorable for the surface to assume a periodic corrugation on a lateral scale of hundreds of nanometers. As a result of this relaxation, strain is decreased in the

neighborhood of the peaks and enhanced in the troughs, Although the roughness observed in the case of $Au/Si_{1-x}Ge_x$ is of a different nature, involving removal of material by diffusion, the same qualitative arguments for variation of strain apply. Partial removal of lateral constraint around high areas allows partial relaxation of strain in these regions, and this relaxation induces strain enhancement in the low areas.

It is necessary to show that the variation of conduction-band splittings derived from BEEM data is consistent with the degree of roughness observed by TEM. Since the strain variation induced by the surface roughness is of arbitrary magnitude and direction, numerical methods were required for this calculation. The lattice-matched $Si_{1-x}Ge_x/Si$ system is described well by elasticity theory[3]; therefore, a finite-element implementation of elasticity was chosen to model the problem, The derived strains in the layer were then used to calculate conduction-band positions and splittings.

The equilibrium strain configuration of the $Si_{1-x}Ge_x$ layer was determined by the solution to a two-dimensional finite-element system. A mesh of triangular elements was used, and a solution was obtained when net force on each element node was equal to zero. This array was used to represent the $Si_{1-x}Ge_x$ layer of our samples, which was nominally 50 nm thick. Periodic boundary conditions were used laterally, with the last node of a row mathematically connected to the first node of the row. A rigid Si substrate lattice was used to fix the bottom row of the grid. Since the degree of roughness was determined by reference to Fig 2b, initial strain in the layer was chosen to be that appropriate for $Si_{0.82}Ge_{0.18}$ lattice-matched to Si. Elastic constants for Si and Ge were linearly interpolated to arrive at constants for the alloy. Strain in the third dimension was fixed at a constant value.

Table I lists the relevant lattice constants *a* and elastic constants for Si and Ge.[19] The derived Poisson ratio v is also shown. Values for $Si_{0.82}Ge_{0.18}$ are linear interpolations.

TABLE I

	Si	Ge	$Si_{0.82}Ge_{0.18}$
a (rim)	0.5431	0.5658	0.5472
c_{11} (Mbar)	1.656	1.285	1.589
c_{12} (Mbar)	0.639	0,483	0.611
C44 (Mbar)	0.795	0.680	0.774
$\nu=c_{12}/(c_{11}+c_{12})$	0.278	0.273	0,278

The lattice constants in Table I yield a bulk value for in-plane uniaxial strain of

$$e_{xx} = (a_{Si} - a_{SiGe}) / a_{SiGe} = -0.749\% \quad (1)$$

with the sign indicating compressive strain. Strain in the third dimension (normal to the grid) was maintained at e_{yy} = -O. 749°/0. Resulting extension in the direction normal to the plane of the layer is

$$e_{zz} = -2 \frac{c_{12}}{c_{11}} e_{xx} = 0.576\%. \quad (2)$$

The finite-element grid was initialized using these values,

In order to calculate band splittings, uniaxial contributions to band positions are calculated. The deformation potential for this contribution is Ξ_u, and the energy shift for a given conduction-band minimum, relative to the weighted average, is[3]

$$E_u^i = \Xi_u\left[\{\hat{a}_i \hat{a}_i\} : \vec{e} - \tfrac{1}{3}(\vec{1} : \vec{e})\right] \tag{3}$$

where $\hat{a}_i$ is the unit vector in the direction of the i^{th} conduction band minimum, and $\{\hat{a}_i \hat{a}_i\}$ represents a dyadic product. Therefore,

$$E_u^x = \Xi_u\left[+\tfrac{2}{3}e_{xx} - \tfrac{1}{3}e_{yy} - \tfrac{1}{3}e_{zz}\right] \tag{4a}$$

$$E_u^y = \Xi_u\left[-\tfrac{1}{3}e_{xx} + \tfrac{2}{3}e_{yy} - \tfrac{1}{3}e_{zz}\right] \tag{4b}$$

$$E_u^z = \Xi_u\left[-\tfrac{1}{3}e_{xx} - \tfrac{1}{3}e_{yy} + \tfrac{2}{3}e_{zz}\right]. \tag{4c}$$

For in-plane compressive strain of the SiGe layer (e_{xx} and e_{yy} negative) energies of [001] minima will in general be raised, and the energies of [100] and [010] minima will be lowered.

It is important to note that, since the observed variation in strain is attributed to surface roughness, all three components of strain will in general be different. This would produce a BEEM spectrum which exhibits three separate thresholds. In practice, however, it is more difficult to reliably resolve three thresholds than two. In order to clearly distinguish the three thresholds, it is necessary to have large strain and also to have the intermediate threshold roughly equidistant between the other two. Since this is a relatively uncommon situation, we have parametrized the spectra in this work with two-threshold fits. While this may underestimate the separation between the highest and lowest of three thresholds, it is unlikely to overestimate,

The deformation potential Ξ_u used for Si and Ge are 9.16 eV and 9.42 eV, respectively.[4] A linear interpolation yields 9.21 eV for $Si_{0.82}Ge_{0.18}$. These deformation potentials are for the A minima, since for $x=0.18$ this minimum is lowest in energy for all values of strain, For $Si_{0.82}Ge_{0.18}$, Eqs. 4 and the interpolated value of Ξ_u yield a bulk value for conduction-band splitting of 122 meV.

The initial modeling of the roughened interface has been performed using a sinusoidal profile for the SiGe surface. The amplitude and period were selected to approximate the profile observed by TEM. SiGe layer thickness as determined from cross-sectional TEM was approximately 56 nm; amplitude and period, A = 2.05 nm and P = 56 nm, respectively, were assigned for the sinusoidal profile. Other amplitude and period values were also investigated.

Figures 4a and 4b show the sinusoidal surface. Using this profile, the finite-element model was used to obtain components of strain at the surface. The strain components e_{xx} and e_{zz} are plotted in Figs. 5b and 5c. Also shown for reference are the bulk values of the strain components. Note that both components of strain are distinctly non-sinusoidal and are not symmetric about the bulk values. Figure 4c shows the conduction-band splitting along the surface, derived from Eqs. 4 using the calculated surface strains. The variation in splitting is from 0.095 eV to 0.144 eV.

Since a two-dimensional model is used for the strain calculation, it is limited to the imposition of a constant strain in the third dimension. However, the roughness at the $Au/Si_{1-x}Ge_x$ interface extends to both lateral dimensions, and the TEM micrograph of Fig. 2b may be thought to represent the typical roughness in any lateral direction. One aim of these calculations is to derive an expected maximum and minimum splitting consistent with the observed roughness. Although the two-dimensional roughness cannot be determined from the TEM images, the effect can be estimated by imposing a constant strain e_{yy} in the other lateral

direction, equal to the maximum or minimum value of e_{xx}, and performing a separate calculation for each case. This procedure yields a slightly increased maximum splitting valueofO.151 eV and a slightly decreased minimum of 0.087 eV; these corrected values are also indicated in Fig. 4c.

In general, the maximum and minimum strains at the surface depend to first order only on the amplitude-to-period ratio (A/P) of the sinusoidal roughness, as long as the strain distortion imposed by the roughness decays sufficiently quickly with depth. In practice this seems to be true for P less than the layer thickness. Several A/P values were modeled, and the results for the maximum and minimum conduction-band splittings are plotted in Fig. 6. It can be seen that the maximum and minimum are not symmetric about the bulk splitting value, a characteristic which is also apparent in Figs. 4 and 5, This is reasonable, since the lateral constraints of elements at the bottom of surface troughs are not directly affected by roughness, but only indirectly by the secondary effect of the relaxation of high areas.

Since the actual surface has areas of larger curvature than the model sinusoidal surface, it is expected that calculations for the actual surface will show a larger range of strains than those for this idealized surface. These calculations are currently underway. In conclusion, the conduction-band splitting of strained Si and $Si_{1-x}Ge_x$ has been directly measured using BEEM spectroscopy. For the case of Ag on $Si_{1-x}Ge_x$, the energy splitting is uniform, with values which agree well with calculations. Deposition of Au on $Si_{1-x}Ge_x$, however, produces a large degree Of spatial heterogeneity in the strain of the $Si_{1-x}Ge_x$ layer. This characteristic is also seen On strained Si, and appears to be due to the intermixing of Au and Si, leading to a roughened interface and heterogeneous strain. The calculated band splittings of an idealized $Si_{1-x}Ge_x$ surface are in reasonable agreement with measured BEEM splittings, indicating that the observed roughness is the probable cause for the variation in observed splittings. Further calculations for a more realistic surface should improve on this agreement. These results emphasize the importance of a characterization and understanding of the completed metal/semiconduct or heterostructure.

The research described in this paper was performed by the Center for Space Microelectronics Technology, Jet Propulsion Laboratory, California Institute of Technology, and was jointly sponsored by the Office of Naval Research and the Ballistic Missile Defense Organization / Innovative Science and Technology Office through an agreement with the National Aeronautics and Space Administration (NASA).

REFERENCES

1. S. C. Jain and W. Hayes, *Semicond. Sci. Technol. 6,547 (1991).*
2. W. J. Kaiser and L. D. Bell, *Phys.* Rev. *Lett.* 60, 1406 (1988); L. D. Bell and W. J. Kaiser, *Phys. Rev. Lett. 61,2368 (1988).* For a more complete review of BEEM, see L. D. Bell, W. J. Kaiser, M. H. Hecht, and L. C. Davis, in ***Scanning Tunneling Microscopy,*** edited by J. A. Stroscio and W. J. Kaiser (Academic Press, San Diego, 1993), pp. 307-348.
3. R. People, *Phys. Rev. B* 32, 1405 (1985).
4. Chris G. Van de Wane and Richard M. Martin, *Phys. Rev. B* 34, 5621 (1986).
5. P. E. Batson and J. F. Morar, *Phys. Rev. Lett. 71,609 (1993).*
6. *G.* Binnig, H. Rohrer, Ch. Gerber, and E. Weibel, *Phys. Rev. Lett. 49,57 (1982).*
7. A. Fernandez, H. D. Hallen, T. Huang, R. A. Buhrman, and J. Silcox, *J. Vac. Sci. Technol. B 9, 590 (1991).*
8. M. Prietsch and R. Ludeke, *Phys. Rev. Lett. 66,2511* (1991).
9. L. D. Bell, M. H. Hecht, W. J, Kaiser, and L. C. Davis, *Phys. Rev. Lett.* 64,2679 (1990).
10. A. M. Milliken, S. J. Manion, W. J. Kaiser, L. D. Bell, and M. H. Hecht, *Phys. Rev. B* 46, 12826 (1992).
11. R. Ludeke, *Phys. Rev. Lett.* 70,214 (1993).
12. A. Bauer, M. T. Cuberes, M. Prietsch, and G. Kaindl, *Phys. Rev. Lett.* 71, 149 (1993).
13. L. D. Bell, A. M. Milliken, S. J. Manion, W. J. Kaiser, R. W. Fathauer, and W. T. Pike, *Phys. Rev, B 50,8082 (1994).*
14. E. Y. Lee and L. J. Schowalter, *Phys. Rev. B* 45,6325 (1992).
15. A. G. Cullis, D. J. Robbins, A. J. Pidduck, and P. W. Smith, ***J. Cryst. Growth* 123, 333 (1992).**
16. A. J. Pidduck, D. J. Robbins, A. G. Cullis, W. Y. Leong, and A. M. Pitt, *Thin Solid Films 222,78 (1992).*
17. M, Hanbucken, Z. Imam, J. J. Metois, and G, LeLay, ***Surf. Sci.* 162,628 (1985).**

18. Z. Ma and L. H. Allen, *Phys.* Rev. *B* 48, 15484 (1993).

19. *CRC* ***Handbook of Materials*** *Science,* ***Vol. III,*** edited by Charles T. Lynch (CRC Press, Cleveland, 1975).

FIGURES

1. (a) Experimental BEEM spectrum of collector current (I_c) versus tunnel voltage for a $Au/Si_{.75}Ge_{.25}/Si(100)$ heterostructure. Tunnel current for this spectrum was 3 nA. The data are shown by circles. Also plotted are two theoretical spectra which have been fit to the data. The first (dashed line) fits only the low-voltage portion ($V < 1.1$ V) with a single threshold; the other fit (solid line) is over a larger range (to 1.6V) using a two-threshold model, The extracted thresholds for the two-threshold fit are separated by about 0.30 V. (b) BEEM I_c-V spectrum, taken on a sample identical to that in (a), showing only a single threshold. Tunnel current for this spectrum was 2 nA. Also plotted is a one-threshold fit to the data (solid line).

2. High-resolution cross-sectional TEM images of $Si_{1-x}Ge_x/Si$ structures. The SiGe/Si interface is out of the field of view in all three images. (a) Image of the as-grown $Si_{.75}Ge_{.25}$ material. (b) Image of a $Si_{.82}Ge_{.18}$ sample with an evaporated Au layer of nominal thickness 10 nm. (c) Image of a $Si_{.82}Ge_{.18}$ sample with 8 nm of evaporated Ag, capped with 8 nm of Au. Nonuniform thinning during sample preparation is responsible for the dark area in the bottom right corner.

3. Conduction-band splitting for $Au/Ag/Si_{1-x}Ge_x/Si(100)$. The experimental points (circles) are derived from the fitted thresholds of the corresponding BEEM spectra. Also plotted (square) is the derived splitting for $Au/Ag/Si(strained)/Si_{1-x}Ge_x(relaxed)$ at $x=.25$. The calculated dependence (line) is from Eqs. 4.

4. (a, b) Sinusoidal surface profile used in elasticity calculations. y=O corresponds to the $Si_{.82}Ge_{.18}/Si$ interface. (c) Calculated conduction-band splitting along this surface, The upper and lower dashed lines represent maximum and minimum values of strain after correction for roughness in two dimensions. The middle dashed line indicates the bulk splitting value.

5. (a) Sinusoidal surface profile used in elasticity calculations, as in Fig. 4b. (b, c) Calculated strain components e_{xx} and e_{zz} along this surface. The dashed lines indicate the bulk values of the strain components.

6, Calculated maximum and minimum splittings at the surface of the $Si_{.82}Ge_{.18}$ layer as a function of amplitude/period ratio (A/P) of the sinusoidal surface roughness. These values have been corrected to estimate the effect of roughness in two dimensions, as described in the text. Also shown for reference is the bulk splitting value (dashed line).

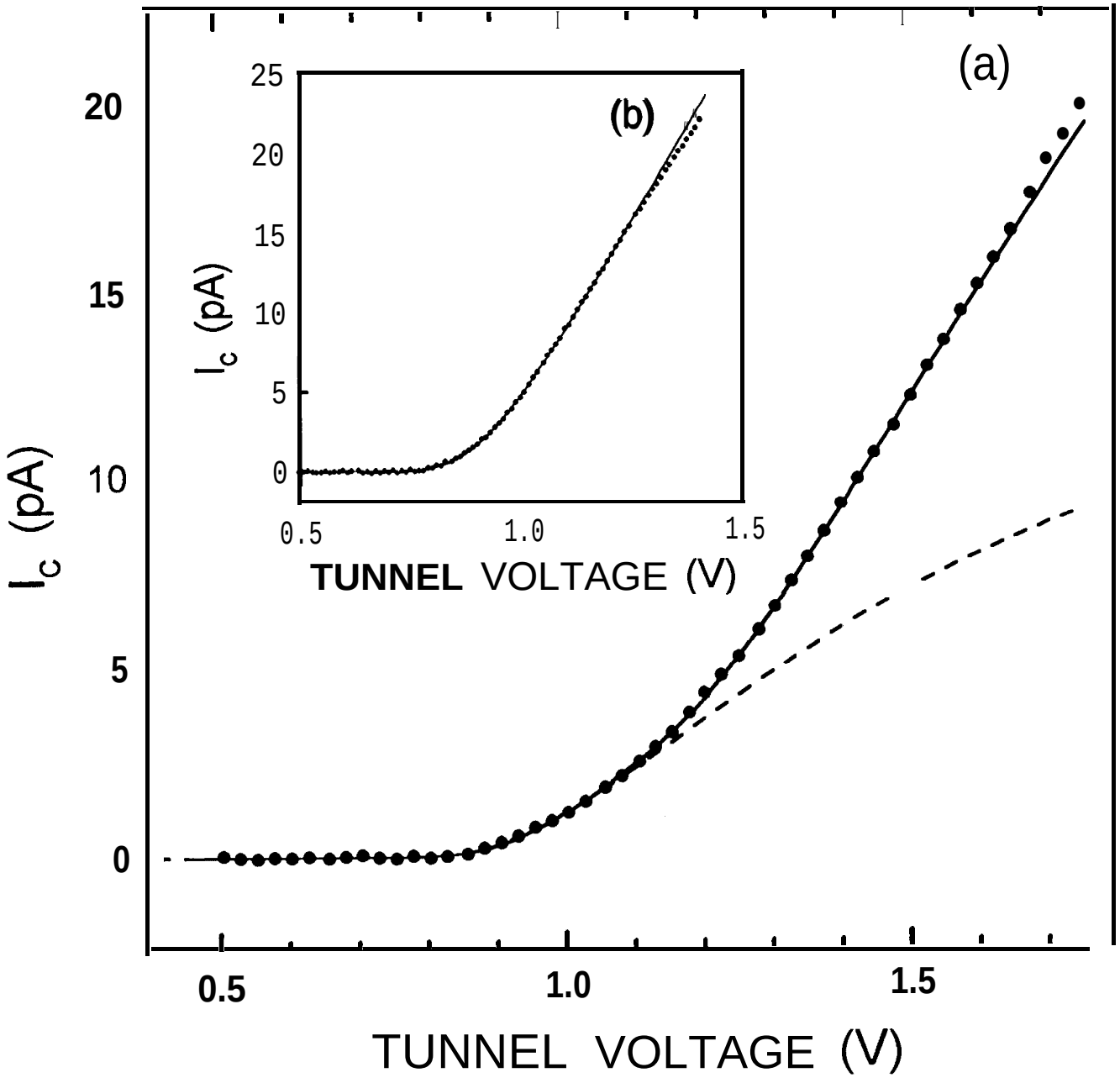
(a)
(b)
20
15
10
5
0
I_c (pA)
0.5
1.0
1.5
TUNNEL VOLTAGE (V)
25
20
15
10
5
0
I_c (pA)
0.5
1.0
1.5
TUNNEL VOLTAGE (V)

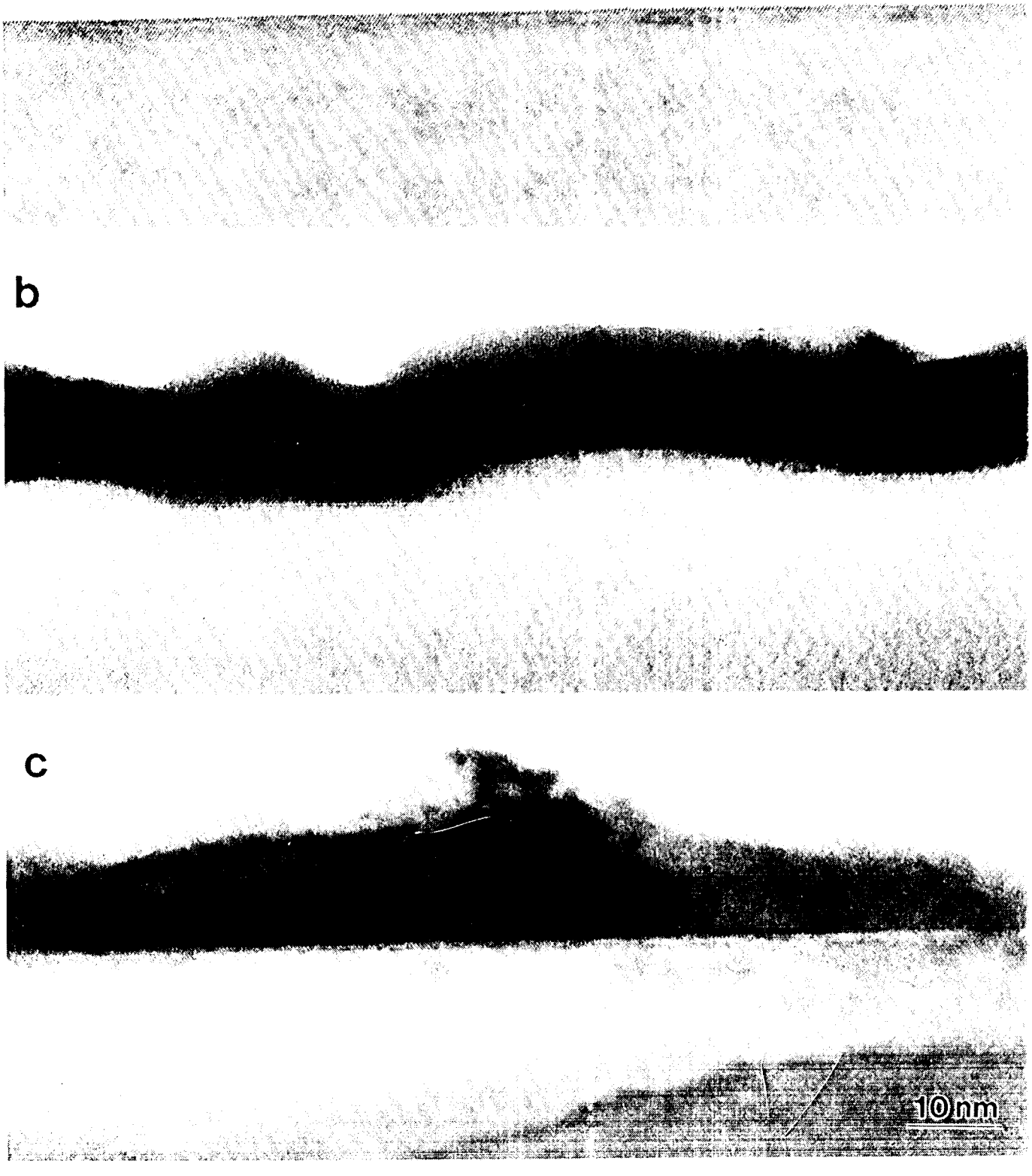
a
b
c
10nm

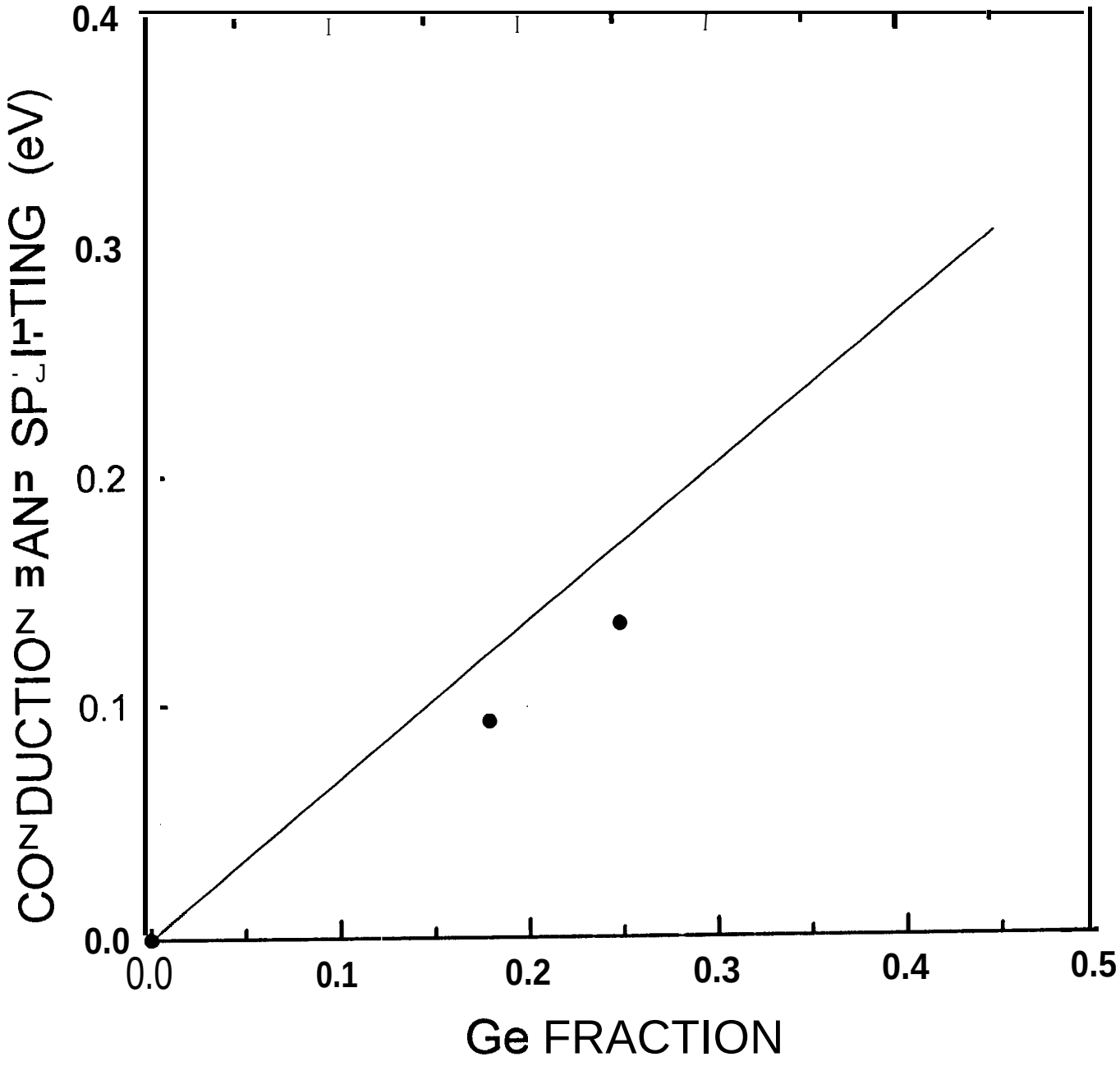
0.4
0.3
0.2
0.1
0.0
0.0
0.1
0.2
0.3
0.4
0.5
Ge FRACTION

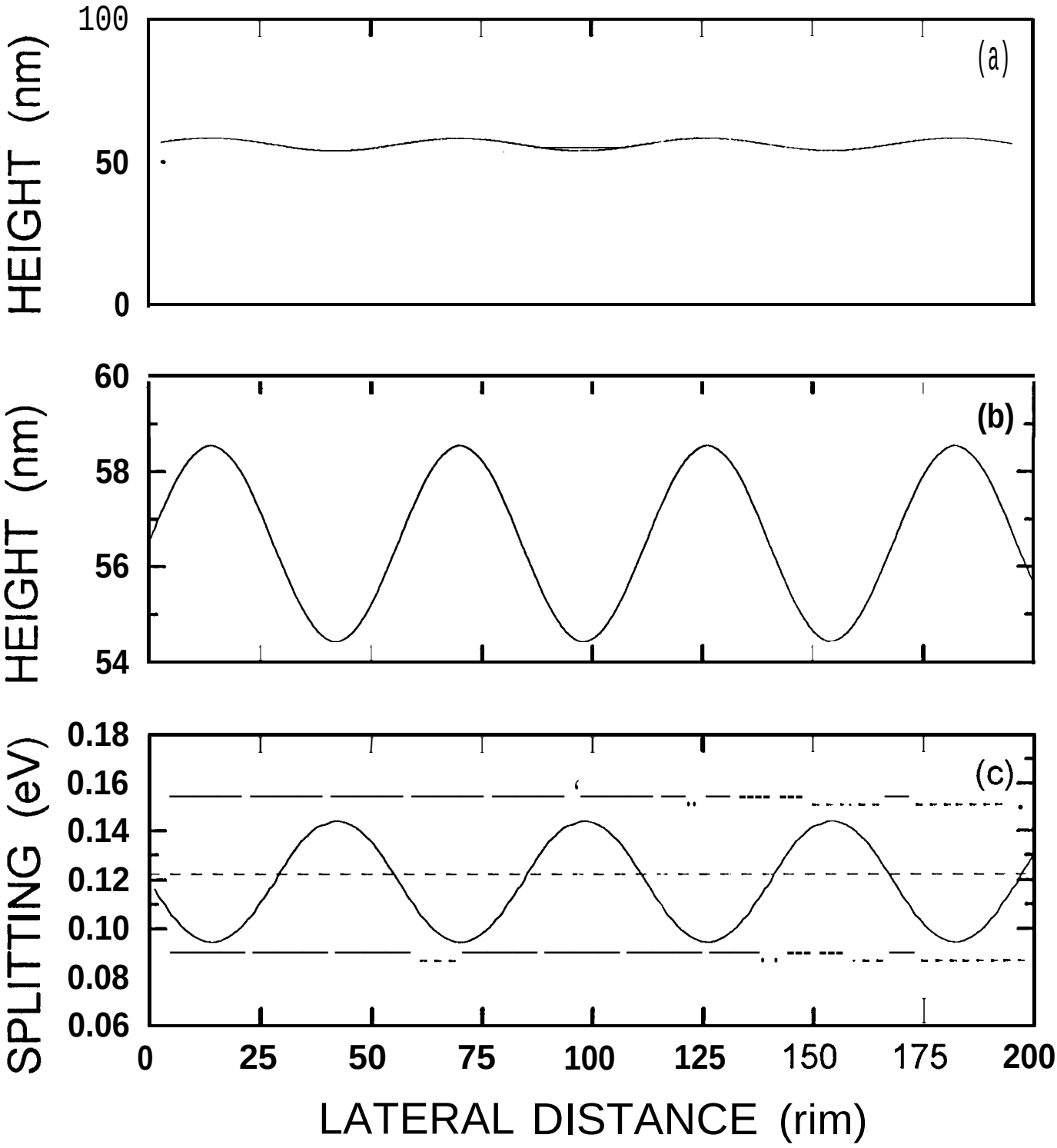
100
50
0
HEIGHT (nm)
(a)
60
58
56
54
HEIGHT (nm)
(b)
0.18
0.16
0.14
0.12
0.10
0.08
0.06
SPLITTING (eV)
(c)
0
25
50
75
100
125
150
175
200
LATERAL DISTANCE (rim)

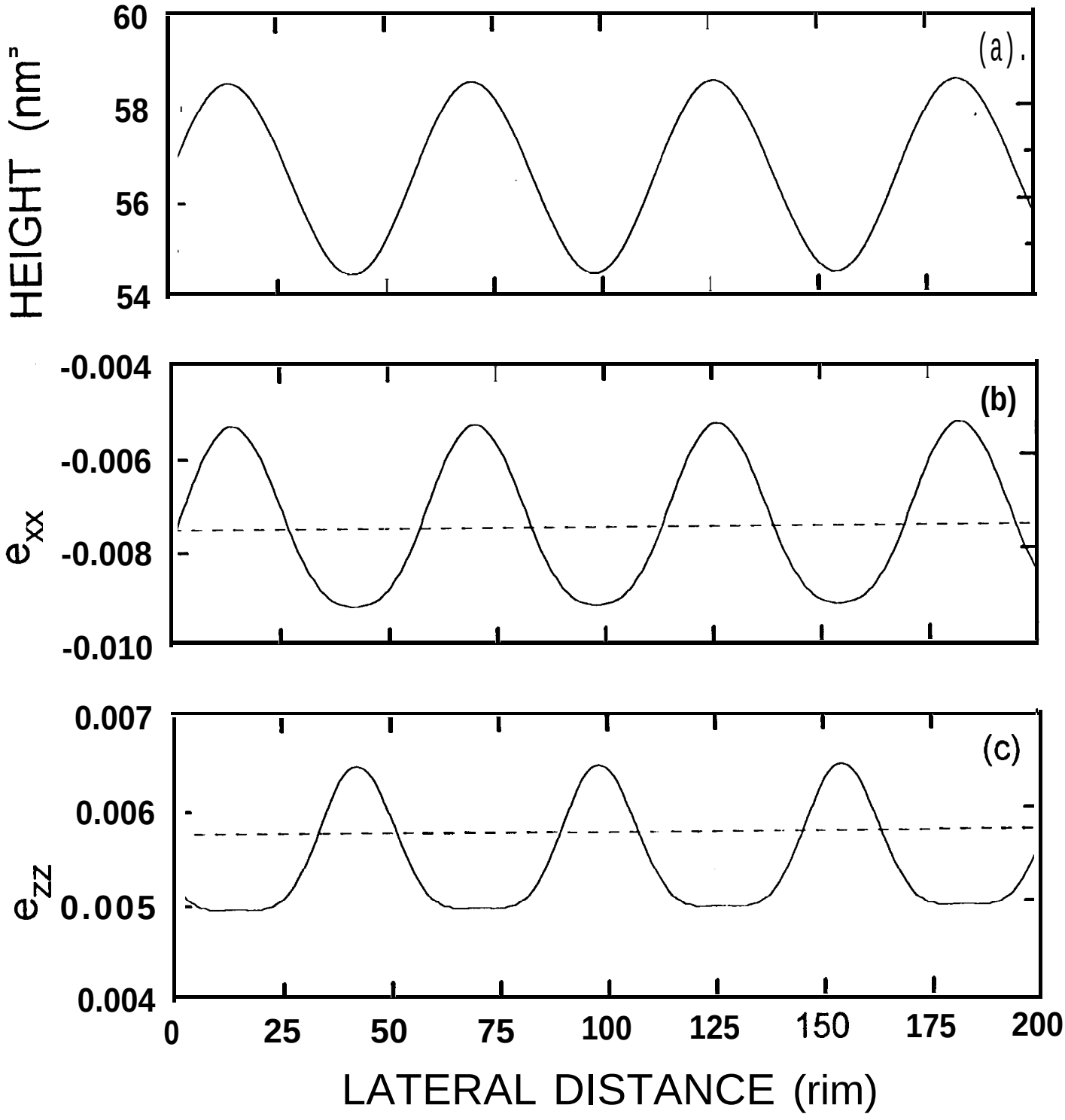
HEIGHT (nm)
60
58
56
54
(a)
e_{xx}
-0.004
-0.006
-0.008
-0.010
(b)
e_{zz}
0.007
0.006
0.005
0.004
(c)
0
25
50
75
100
125
150
175
200
LATERAL DISTANCE (rim)

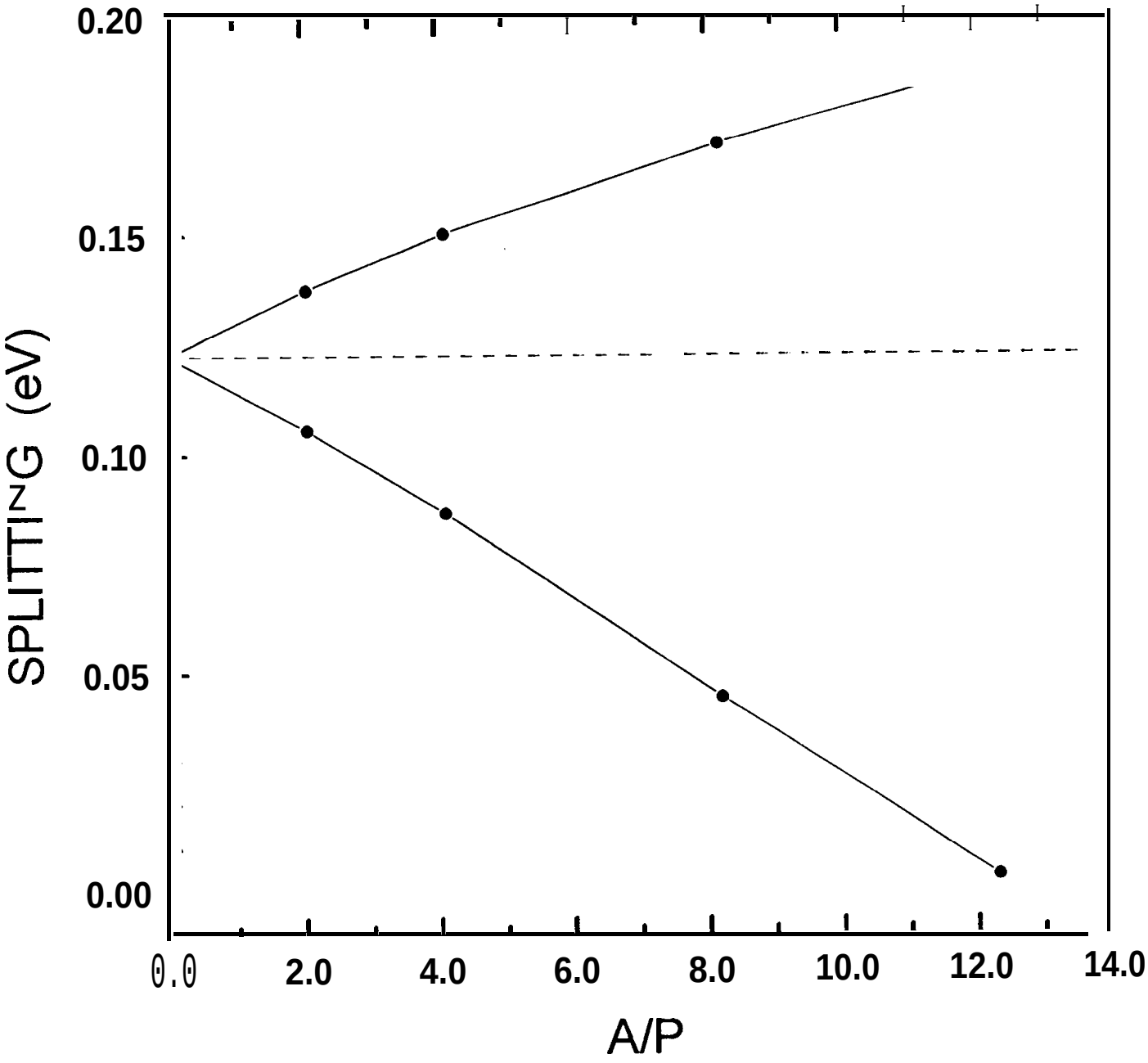
0.20
0.15
0.10
0.05
0.00
SPLITTING (eV)
0.0
2.0
4.0
6.0
8.0
10.0
12.0
14.0
A/P